Available online at www.sciencedirect.com
ScienceDirect
Thermochimica Acta 451 (2006) 10–15
thermochimica acta
www.elsevier.com/locate/tca

Thermal kinetic analysis of InN by TG–MS combined with PulseTA

Hui-Mei Yu [a,*], Qing-Hong Zhang [b], Ling-Jun Qi [a], Chang-Wei Lu [a], Tong-Geng Xi [a], Lan Luo [a]

[a] *Analysis & Testing Center for Inorganic Materials, Shanghai Institute of Ceramics, Chinese Academy of Sciences, 1295 Dingxi Rd., 200050 Shanghai, PR China*
[b] *State Key Laboratory of High Performance Ceramics and Superfine Structure, Shanghai Institute of Ceramics, Chinese Academy of Sciences, 1295 Dingxi Rd., 200050 Shanghai, PR China*

Received 13 March 2006; received in revised form 20 July 2006; accepted 23 July 2006
Available online 28 July 2006

Abstract

The present work was to determine the optimal nitridation conditions of InN prepared by the nitridation of In_2O_3 with NH_3 gas at 550–600 °C for 5–8 h. Thermogravimetry–mass spectrometry (TG–MS) coupling technique was used for a simultaneous characterization of the changes of mass and determination of the evolved gases during the thermal decomposition of InN prepared at the different nitridation temperatures. Moreover, pulse thermal analysis (PulseTA) was combined with TG–MS for the quantitative calibration of the evolved nitrogen formed during the thermal decomposition of InN samples. The decomposition of InN under argon atmosphere was found to occur in a single-stage reaction at 550–750 °C with indium and N_2 as final product. It was confirmed that the optimal nitridation condition of InN should be at 600 °C for 8 h by the nitridation of In_2O_3 with NH_3 gas. The thermal kinetic TG analysis of InN under argon atmosphere was studied at the heating rate of 5, 10, 15, 20 K min^{-1}. The activation energy (E_a) and the pre-exponential factor ($\log A$) were obtained by means of ASTME698, Friedman and Ozawa–Flynn–Wall (FWO) methods. The most probable conversion function $f(\alpha)$ was found.

Keywords: Thermal decomposition; Kinetic analysis; InN; TG–MS; PulseTA

1. Introduction

Indium nitride (InN) is an important III-nitride semiconductor with many potential applications [1]. During the last few years, various methods for the growth of InN have been used, such as reactive sputtering deposition, metal organic vapor phase epitaxy, microwave-excited metal organic vapor phase epitaxy, pulse discharge and molecular beam epitaxy, etc. [2–6]. There have been significant improvements in the growth of InN films. Gao et al. [7] reported a novel method for the synthesis of InN powders by the direct nitridation of In_2O_3 nanoparticles. The InN powders were characterized by X-ray diffraction (XRD), field emission scanning electron microscopy (FE-SEM), transmission electron microscopy (TEM), thermogravimetry–differential scanning calorimetry (TG–DSC) and Brunauer–Emmett–Teller (BET) surface area techniques. The influence of reaction temperature on the lattice parameters of InN powders formed by nitridation of In_2O_3 was studied. They found that nanosized In_2O_3 was completely converted into InN at 600 °C within 8 h. Moreover, the nitrogen content of the InN powder, detected by CHN elemental analysis, was consistent with the theoretical value, but the TG curve showed that the mass loss (11.24%) was slightly higher than the theoretical content of pure InN (10.86%). In order to determine the optimal nitridation conditions, the InN samples, prepared by the nitridation of In_2O_3 with NH_3 gas at 550 °C for 8 h, 580 °C for 5 h and 600 °C for 8 h, were studied by TG–MS combined with PulseTA techniques. TG–MS [8–11] was useful for a simultaneous characterization of the mass changes and the evolved gaseous products. The PulseTA technique was applied for quantitative calibration of mass spectrometric signals in the combined TG–MS system [12,13]. Moreover, we studied the kinetics of thermal decomposition of InN by TG analysis, and compared the results with those of the Ambacher et al. [14]. Ambacher et al. studied the thermal stability and desorption of InN prepared by metal organic chemical vapor

* Corresponding author. Tel.: +86 21 52413404.
E-mail address: huimeiyu@mail.sic.ac.cn (H.-M. Yu).

0040-6031/$ – see front matter © 2006 Elsevier B.V. All rights reserved.
doi:10.1016/j.tca.2006.07.014

deposition. In order to determine the effective decomposition activation energy, the nitrogen flux was calculated from the measured nitrogen pressure. The rate of N evolution is equal to the rate of decomposition and the slope of $\ln[\varphi(N)]$ versus to $1/T$ gives the effective activation energy of the decomposition in vacuum E_{MN}. They reported that the effective activation energy for nitrogen decomposition in vacuum was 3.48 eV (336 kJ/mol) for InN. The studies on the thermal behavior of InN have been seen in the literatures [1,15–17]. In our work, the dependence of the activation energy and the pre-exponential factor for the InN decomposition on the conversion variable was obtained using the Friedman and the FWO methods, respectively. We also studied the mechanism of thermal decomposition of the InN powder using non-isothermal analysis techniques.

2. Experimental

2.1. Thermal analysis

InN samples were prepared by the nitridation of In_2O_3 with NH_3 gas at 550 °C for 8 h, 580 °C for 5 h and 600 °C for 8 h. Indium nitrate (99.5% $In(NO_3)_3{\cdot}4.5H_2O$) solution with concentration of 0.3 mol/L was used as the main raw material. Firstly, the aqueous solution was neutralized to pH 8 with the ammonia solution of 1.0 mol/L at room temperature. The precipitate was separated from the solution by filtration, and repeatedly washed with distilled water. Then, the white filtration cake was dried at 110 °C for 24 h, and calcined at 450 °C for 2 h to obtain crystalline In_2O_3 nanoparticles. The In_2O_3 powders were placed in a high-purity quartz boat and set in a quartz tube furnace (inner diameter of 82 mm) with air-tight end gaskets. The reactor was flushed with argon to eliminate oxygen in the system during the heat-up period. As the temperature reached 500 °C, NH_3 (99.9% purity) was introduced from one end of the reactor at the flow rate of 0.5 L min^{-1}. The furnace was heated to the experimental reaction temperature (500–600 °C) at the rate of 10 °C min^{-1}. The temperature was subsequently kept constant for 5–8 h, and then the sample was cooled to room temperature at approximately 6 °C min^{-1} in an ammonia atmosphere.

A Netzsch STA 449C TG–DSC thermoanalyzer coupled with a Balzers Thermostar Quadrupole Mass Spectrometer was used in the experiments. A quartz capillary was used as the interface between thermoanalyzer and the quadrupole MS. TG–MS combined with PulseTA was used for the quantification of the amount of N_2 formed during InN decomposition. For calibration pure nitrogen (99.999%) was used. Each injection volume of nitrogen was 0.5 mL and nitrogen for the calibration was injected three times during the experiments. For the kinetic analysis, the masses of InN prepared by the nitridation of In_2O_3 at 600 °C for 8 h were 20.30, 15.43, 11.55 and 16.69 mg, separately. The TG heating rates were 5, 10, 15, 20 K min^{-1}, respectively. Argon at a flow rate of 20 mL min^{-1} was used as the carrier gas. The temperature range was from room temperature to 900 °C.

2.2. Kinetic analysis

The commonly used kinetic equation of solid thermal decomposition under non-isothermal conditions is given as follows:

$$\frac{d\alpha}{dT} = \left(\frac{1}{\beta}\right) k(T) f(\alpha)$$

where α is the extent of reaction, $k(T) = A\,e^{-E_a/RT}$, E_a is the activation energy, A the pre-exponential factor and β the heating rate. $f(\alpha)$ is the differential conversion function. Non-isothermal kinetic analyses were used in our experiments using the kinetics software from Netzsch.

3. Results and discussion

3.1. The optimal nitridation conditions of InN by TG–MS–PulseTA measurements

In order to determine the optimal nitridation conditions, the InN samples prepared by the nitridation of In_2O_3 with NH_3 gas at 550–600 °C for 5–8 h were studied by TG–MS combined with PulseTA techniques. Fig. 1 shows the TG–DTG–MS curves of InN prepared by the nitridation of In_2O_3 with NH_3 gas at 550 °C for 8 h, 580 °C for 5 h and 600 °C for 8 h. For the InN powder obtained by the nitridation of In_2O_3 at 550 °C for 8 h, the TG results in Fig. 1(b) show that the mass loss was 0.63 mg at 550–750 °C (about 2.72%). The derivative thermogravimetry (DTG) curve shows the maximum of the peak at 686 °C. The MS signal recorded during the nitridation of In_2O_3 at 550 °C for 8 h decomposition in Fig. 1(a) shows the N_2^+ ($m/z = 28$) ion peak in the range of 550–750 °C (peak at 689 °C). The integral intensity of the N_2^+ ($m/z = 28$) was 4.75E−07 A s. The mean value of the integral intensities of the injected pulses of nitrogen (0.5 mL, temperature of injection 20 °C) was 5.476E−07 A s. Therefore, the amount of N_2 formed during the nitridation of In_2O_3 at 550 °C for 8 h decomposition calculated from these data corresponds to 0.51 mg. The mass of the product of nitridation of In_2O_3 at 550 °C for 8 h was 23.02 mg. The stoichiometric amount of nitrogen from the decomposition of nitridation of In_2O_3 at 550 °C for 8 h was 2.50 mg. The measured values by TG and PulseTA results were lower than the stoichiometric value.

In Fig. 1(d), the TG result shows that the mass loss of InN obtained by the nitridation of In_2O_3 at 580 °C for 5 h was 0.71 mg at 550–750 °C (about 3.62%). The DTG curve shows the maximum of the peak at 684 °C. In Fig. 1(c), the N_2^+ ($m/z = 28$) ion peak (at 685 °C) closely corresponds to that given from the DTG curve. The amount of N_2 formed during the decomposition of the product of nitridation of In_2O_3 at 580 °C for 5 h calculated from these data corresponds to 0.59 mg. The stoichiometric amount of nitrogen from the decomposition of 19.55 mg nitrided In_2O_3 at 580 °C for 5 h was 2.13 mg. The measured values by TG and PulseTA results were lower than the stoichiometric value. Therefore, the nanosized In_2O_3 was partially converted into InN at 550 °C for 8 h and 580 °C for 5 h.

For the InN powder prepared by the nitridation of In_2O_3 at 600 °C for 8 h, the TG and DTG curves are shown in Fig. 1(f). The TG result shows that the mass loss was 3.56 mg

Table 1
The PulseTA results for the InN powders obtained under different nitridation conditions

Nitridation condition	Sample mass mg	N_2 pulse 1, $\times 10^{-7}$ A s	N_2 pulse 2, $\times 10^{-7}$ A s	N_2 pulse 3, $\times 10^{-7}$ A s	Average N_2 pulse/10^{-7} A s	Decomposed N_2/10^{-7} A s	Stoichiometric amount of nitrogen/mg	Measured amount of nitrogen/mg	Conversion of In_2O_3 (%)
550 °C, 8 h	23.02	5.547	5.474	5.406	5.476	4.75	2.50	0.51	20
580 °C, 5 h	19.55	5.789	5.569	5.598	5.652	5.709	2.13	0.59	28
600 °C, 8 h	34.38	9.214	8.795	8.645	8.885	55.60	3.74	3.65	98

Note: Pulse volume = 0.5 ml and injection temperature is at 20 °C.

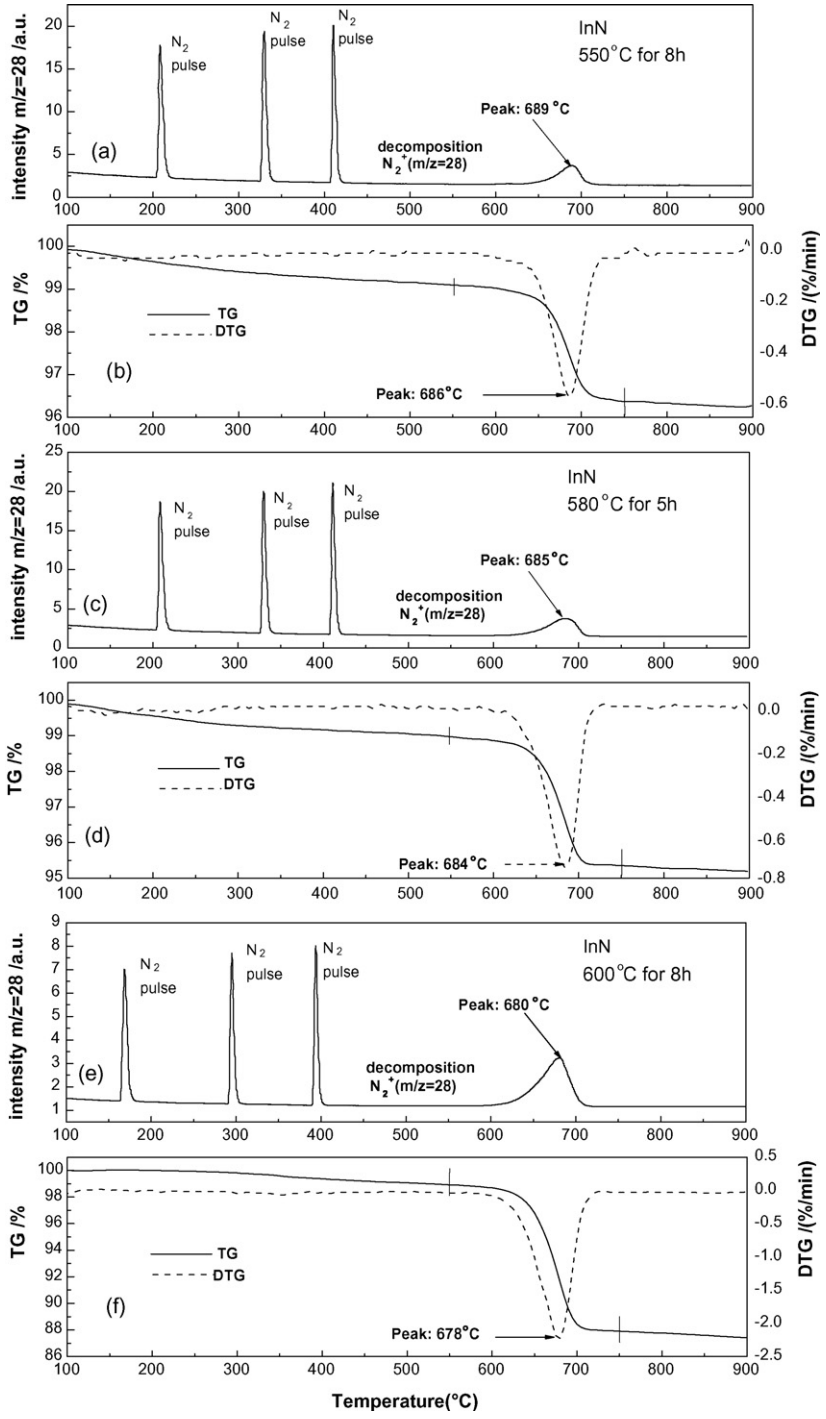

Fig. 1. (a–f) The TG–DTG–MS curves of InN prepared by the nitridation of In_2O_3 with NH_3 gas at 550 °C for 8 h, 580 °C for 5 h and 600 °C for 8 h.

at 550–750 °C (about 10.36%). The mass of the product of the nitridation of In_2O_3 at 600 °C for 8 h was 34.38 mg. The stoichiometric amount of nitrogen from the decomposition of the product of the nitridation of In_2O_3 at 600 °C for 8 h was 3.74 mg. The theoretical value of the mass loss was 10.88%. The measured value (10.36%) by TG was close to the stoichiometric value. The DTG curve shows the maximum of the peak at 678 °C. The N_2^+ ($m/z = 28$) ion mass spectrometric peak (at 680 °C) in Fig. 1(e) closely corresponds to that observed from the DTG curve. The amount of N_2 formed during the decomposition of the product of the nitridation of In_2O_3 at 600 °C for 8 h calculated from these data corresponds to 3.65 mg. The measured value (3.65 mg) by PulseTA result was close to 3.74 mg of the stoichiometric value. The PulseTA results of the studies of InN decomposition under different nitridation conditions are listed in Table 1. The results indicate that about 20 and 28% nanosized In_2O_3 were converted into InN at 550 °C for 8 h and 580 °C for 5 h, respectively. The amount of evolved nitrogen in the experiments, measured by the TG–MS–PulseTA method, equals to ca. 98% of the amount of the nitrogen that should be present in the InN at 600 °C for 8 h. The missing ca. 2% amount of the nitrogen may have resulted from an oxidized surface shell. From Table 1, it is clear that with the different nitridation temperature, the conversion of In_2O_3 is also changed. Moreover, the maxima peak temperatures for the decomposition of InN obtained from MS curves at the 600, 580 and 550 are 680, 685 and 689 °C, separately. Therefore, the thermal decomposition temperature becomes higher as we increase the oxygen level. In addition, we have found that the particle size affect on the thermal decomposition of InN (please see ref. [15]). In general, both initial and final thermal decomposition temperature decreased with decreasing of particle size of the sample. In our experiments, nanoparticles of InN was used for the TG–MS–PTA analysis. For example, for 600 °C the size is 40–300 nm, and InN of a much finer crystallite size was obtained by the nitridation at a lower temperature. The PulseTA results showed that the nanosized In_2O_3 was almost completely converted into InN at 600 °C for 8 h. Moreover, carbon, hydrogen and nitrogen (CHN) element analysis was carried out on an Elementar Vario EL element analysis instrument, and pure oxygen was introduced to assure the nitride solid was combusted completely. The nitrogen content of In_2O_3 nanoparticles nitride at 600 °C for 8 h is 10.82%, which is consistent with the theoretical value of 10.86% [7]. Therefore, the optimal nitridation conditions of InN, prepared by the nitridation of In_2O_3 with NH_3 gas, should be at 600 °C for 8 h. Some scientists have made a lot of work on the preparation of InN [18–21]. We think the temperature for the preparation of InN can be above 680 °C from the In_2O_3. However, the conversion In_2O_3 to InN is very sensitive to the nitridation temperature and reaction time. We also obtained the InN powder by the nitridation of ammonia at above 650 °C. When the nitridation temperature was higher than 650 °C, black droplet of indium metal could be seen in the resultant powder by the naked eye. Therefore, the pure InN can be prepared in a relatively narrow temperature range (580–620 °C) in the ref. [7]. Based on the XRD and CHN analysis, no impurity was detected. The purity of NH_3 of 99.9% may be pure enough to obtain high-purity of InN. It is also notable that we used a relative high flow rate of 500 mL min^{-1}. The optimal nitridation conditions of InN should be at 600 °C for 8 h. It showed that TG–MS combined with PulseTA technique offers a good tool for the quantification of the evolved nitrogen in the InN powder.

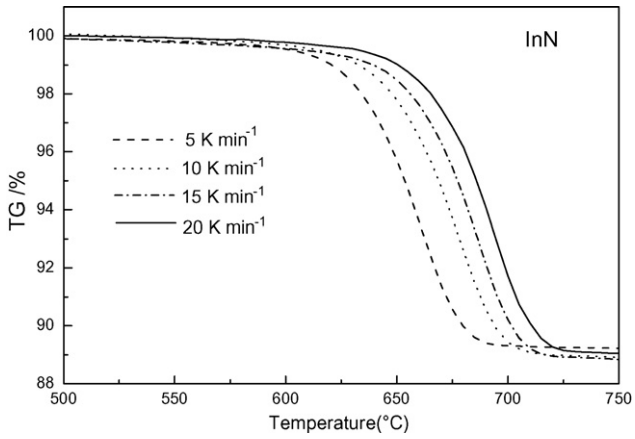

Fig. 2. The TG curves of InN in argon at heating rates of 5, 10, 15, 20 K min^{-1}.

3.2. TG-kinetic analysis of the InN decomposition

The InN powder obtained by the nitridation of In_2O_3 at 600 °C for 8 h was used for the thermal TG-kinetics analysis. Fig. 2 shows the TG curves of InN under argon atmosphere at the heating rate of 5, 10, 15, 20 K min^{-1}. The TG signals indicate that the mass loss between 550 and 750 °C was completed in one step. The DTG curves at the heating rate of 5, 10, 15, 20 K min^{-1} are depicted in Fig. 3. The DTG curves show the peak maxima at 661, 678, 688 and 695 °C, respectively. The ASTME698, Friedman and Ozawa–Flynn–Wall methods can calculate the obtained activation energy and log A of the decomposition process under non-isothermal conditions. Fig. 4 shows the average activation energy and log A obtained by the ASTME698 method for the decomposition of InN in argon. The activation energies and log A obtained are 249 ± 1.2 kJ/mol and 11.46 s^{-1}, respectively. The value of E_α calculated by ASTME698 was lower than the value of 336 kJ/mol reported [14]. The use of multiple heating rate experiments eliminates the need to determine

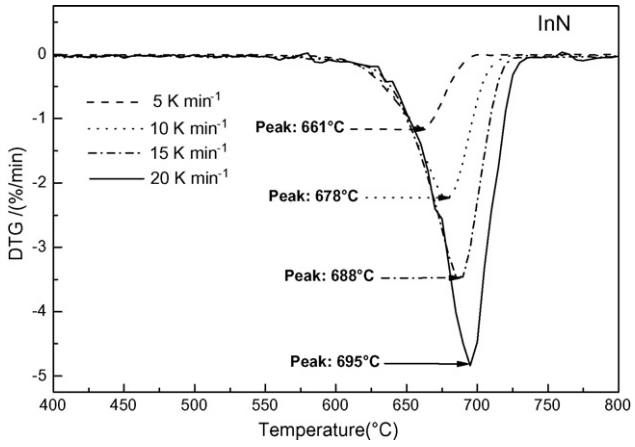

Fig. 3. The DTG curves of InN at heating rates of 5, 10, 15, 20 K min^{-1}.

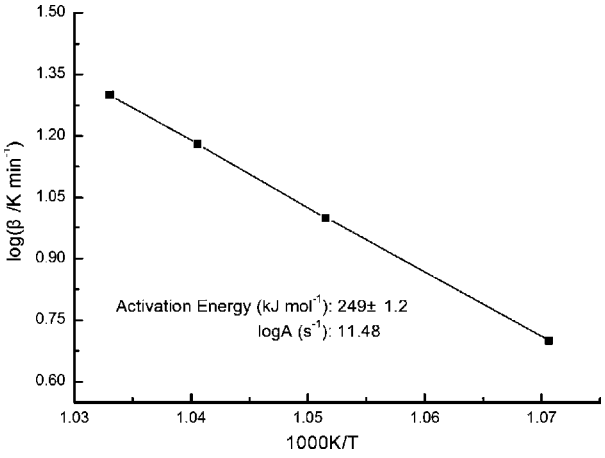

Fig. 4. The activation energy and log A obtained by the ASTME698 method for the thermal decomposition of InN in argon.

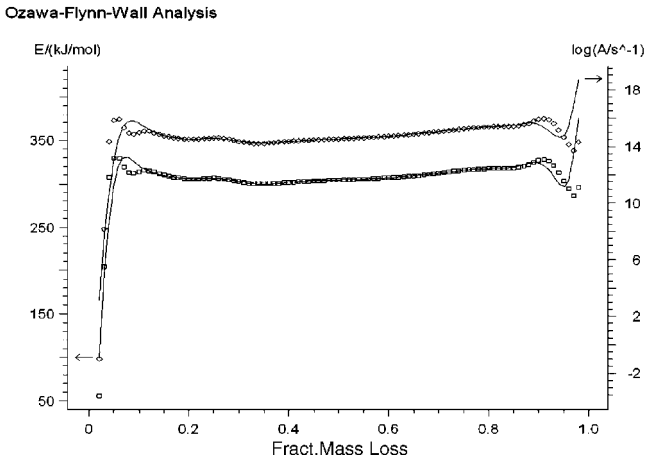

Fig. 6. The dependence of E_a and log A obtained by Ozawa–Flynn–Wall analysis for the thermal decomposition of InN in argon on the extent of reaction, α.

the kinetic model, using the Friedman and the FWO methods to calculate the activation energy. The estimated values of the E_a and log A for the InN decomposition given by both methods are shown in Figs. 5 and 6. The dependence of E_α and log A on the extent of conversion α, calculated by the two methods, is shown in Table 2. The results show that the value of E_a and log A calculated by the Friedman method varied with α (Fig. 5) because the calculation method is very sensitive to experimental noise. But the FWO method used in Fig. 6 shows that the activation energies and log A are almost constant with α [22,23]. It suggested that the thermal decomposition of InN take place in one step that probably obeys a single kinetic mechanism [24]. Murali et al. [25] reported that a kinetic study of indium formation from indium oxide powder. The kinetics for the reaction was determined quantitatively from the X-ray powder diffraction data. The activation energy for the formation reaction of InN and the Avrami constant was obtained in the temperature range of 580–650 °C. In our work, we obtained the activation energy and pre-exponential factor for the thermal decomposition of InN in argon on the extent of reaction. A comparison between the two results was different. Fig. 7 is the best fit of TG measurements for the decomposition of InN, simulated with reaction type F1 for heating rates of 5, 10, 15 and 20 K min^{-1}. The signs represent the measured data. The solid lines are the

Table 2
Activation energies calculated using two methods during the decomposition of InN at multiple-scan rate

Extent of conversion, α	Friedman method		FWO method	
	E_a (kJ/mol)	log A (s^{-1})	E_a (kJ/mol)	log A (s^{-1})
0.02	154 ± 111	5.29	55 ± 192	−0.99
0.05	287 ± 22	13.31	330 ± 123	15.82
0.10	293 ± 11	13.78	314 ± 32	14.96
0.20	299 ± 7	14.21	306 ± 16	14.50
0.30	278 ± 15	13.08	302 ± 11	14.35
0.40	314 ± 19	15.13	302 ± 8	14.34
0.50	313 ± 12	15.15	304 ± 6	14.52
0.60	327 ± 16	15.96	307 ± 6	14.70
0.70	342 ± 18	16.79	312 ± 6	15.04
0.80	340 ± 15	16.68	318 ± 8	15.37
0.90	340 ± 19	16.66	327 ± 9	15.90
0.95	340 ± 47	16.64	303 ± 18	14.61
0.98	376 ± 101	18.46	296 ± 34	14.29

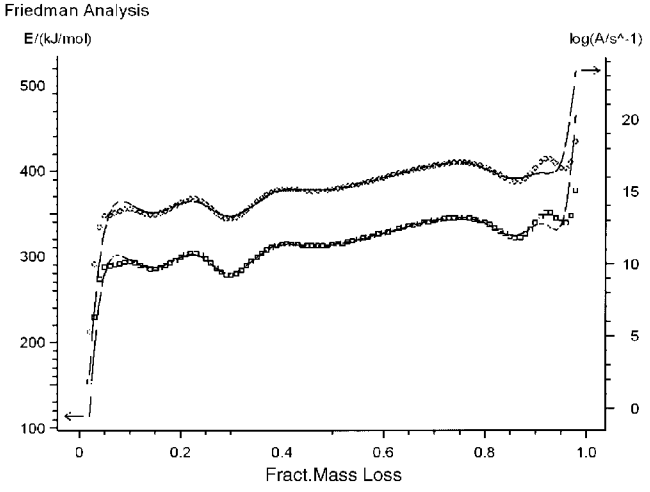

Fig. 5. The dependence of E_a and log A obtained by Friedman analysis for the thermal decomposition of InN in argon on the extent of reaction, α.

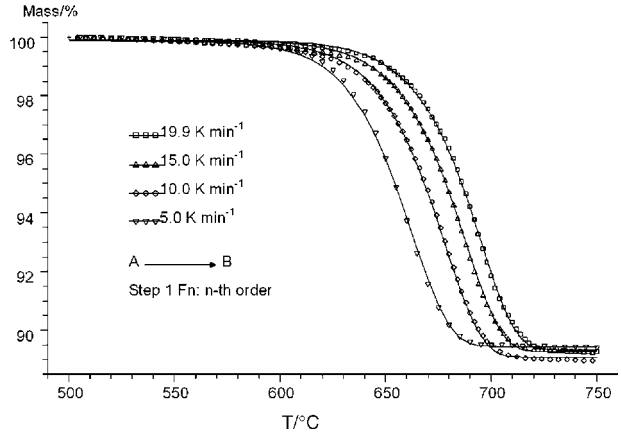

Fig. 7. The best fit of TG measurements for the decomposition of InN, simulated with reaction type F1 for the heating rates 5, 10, 15 and 20 K min^{-1}. The signs represent the measured data. The solid lines are the fitted curves.

fitted curves. The correlation coefficient is 0.9994. The decomposition of InN under argon atmosphere was thus found to occur in a first-order reaction (type F1) at 550–750 °C.

4. Conclusions

The experimental results for the thermal decomposition of InN in argon by TG–MS combined with PulseTA technique showed that the optimal nitridation conditions of InN, prepared by the nitridation of In_2O_3 with NH_3 gas, should be at 600 °C for 8 h. The average activation energy and $\log A$ calculated by ASTME 698 are 249 ± 1.2 kJ/mol and $11.46\,s^{-1}$, respectively. The dependences of E_a and $\log A$ for the InN decomposition on the extent of conversion α by the Friedman method and the FWO method were obtained, separately. The most probable conversion function, $f(\alpha)$, for the decomposition of InN in argon with N_2 as gaseous product at 550–750 °C was one step with reaction type F1.

Acknowledgement

The authors are grateful for the support by the National Natural Science Foundation of China (no. 50372079).

References

[1] A.G. Bhuiyan, A. Hashimoto, A. Yamamoto, J. Appl. Phys. 94 (2003) 2779–2808.
[2] R.T. Shamrell, C. Parman, Opt. Mater. 13 (1999) 289–292.
[3] N. Yoshimoto, T. Matsuoka, T. Sasaki, A. Katsui, Appl. Phys. Lett. 59 (1991) 2251–2253.
[4] Q.X. Guo, M. Nishio, H. Ogawa, A. Wakahara, A. Yoshida, Phys. Rev. B 58 (1998) 15304–15306.
[5] M.-C. Lee, H.-C. Lin, Y.-C. Pan, C.-K. Shu, J. Ou, W.-H. Chen, W.-K. Chen, Appl. Phys. Lett. 73 (1998) 2606–2608.
[6] H. Lu, W.J. Schaff, J. Hwang, H. Wu, W. Yeo, A. Pharkya, L.F. Eastman, Appl. Phys. Lett. 77 (2000) 2548–2550.
[7] L. Gao, Q.H. Zhang, J.G. Li, J. Mater. Chem. 13 (2003) 154–158.
[8] C.W. Lu, T.G. Xi, Thermal Analysis and Mass Spectrometry, Shanghai Science and Technology Publishing House, China, 2002.
[9] C.W. Lu, Y.F. Zhang, X.H. Yang, Y.X. Chen, T.G. Xi, J.K. Guo, J. Thermal. Anal. 45 (1995) 227–233.
[10] C.W. Lu, Z. He, T.G. Xi, Y.X. Chen, L. Luo, Thermochim. Acta 334 (1999) 149–155.
[11] C.W. Lu, Q. Wang, Y.X. Chen, J.L. Shi, Thermochim. Acta 404 (2003) 65–70.
[12] M. Maciejewski, C.A. Muller, R. Tschan, W.D. Emmerich, A. Baiker, Thermochim. Acta 295 (1997) 167–182.
[13] M. Maciejewski, A. Baiker, Thermochim. Acta 295 (1997) 95–105.
[14] O. Ambacher, M.S. Brandt, R. Dimitrov, T. Metzger, M. Stutzmann, R.A. Fischer, A. Miehr, A. Bergmaier, G. Dollinger, J. Vac. Sci. Technol. B 14 (1996) 3532–3542.
[15] H.M. Yu, Q.H. Zhang, L.J. Qi, C.W. Lu, T.G. Xi, L. Luo, Thermochim. Acta 440 (2006) 195–199.
[16] B. Onderka, J. Unland, R. Schmid-Fetzer, J. Mater. Res. 17 (12) (2002) 3065–3083.
[17] M.R. Ranade, F. Tessier, A. Navrotsky, R. Marchand, J. Mater. Res. 16 (10) (2001) 2824–2831.
[18] B. Schwenzer, L. Loeffler, R. Seshadri, S. Keller, F.F. Lange, S.P. DenBaars, U.K. Mishra, J. Mater. Chem. 14 (2004) 637–641.
[19] S. Vaddiraju, A. Mohite, A. Chin, M. Meyyappan, G. Sumanasekera, B.W. Alphenaar, M.K. Sunkara, Nano Lett. 5 (8) (2005) 1625–1631.
[20] T. Tao, S. Han, W. Jin, X. Liu, C. Li, D. Zhang, C. Zhou, B. Chen, J. Han, M. Meyyapan, J. Mater. Res. 19 (2) (2004) 423–426.
[21] S. Luo, W. Zhou, Z. Zhang, X. Dou, L. Liu, X. Zhao, D. Liu, L. Song, Y. Xiang, J. Zhou, S. Xie, Chem. Phys. Lett. 411 (2005) 361–365.
[22] D. Zhan, C. Cong, K. Diakite, Y. Tao, K. Zhang, Thermochim. Acta 430 (2005) 101–105.
[23] K. Zhang, J. Hong, G. Cao, D. Zhan, Y. Tao, C. Cong, Thermochim. Acta 437 (2005) 145–149.
[24] J. Opfermann, J. Thermal. Anal. 60 (2000) 641–658.
[25] A.K. Murali, A.D. Barve, S.H. Risbud, Mater. Sci. Eng. B 96 (2002) 111–114.